

Liquid crystal hyperbolic metamaterial for wide-angle negative-positive refraction and reflection

G. Pawlik,^{1, a)} K. Tarnowski,¹ W. Walasik,² A.C. Mitus,¹ and I.C. Khoo³

¹⁾*Institute of Physics, Wroclaw University of Technology, Poland*

²⁾*Aix Marseille Universite, Institut Fresnel, France*

³⁾*Department of Electrical Engineering, Pennsylvania State University, USA*

We show that nanosphere dispersed liquid crystal (NDLC) metamaterial can be characterized in near IR spectral region as an indefinite medium whose real parts of effective ordinary and extraordinary permittivities are opposite in signs. Based on this fact we design a novel electrooptic effect: external electric field driven switch between normal refraction, negative refraction and reflection of TM incident electromagnetic wave from the boundary vacuum/NDLC. A detailed analysis of its functionality is given based on effective medium theory combined with a study of negative refraction in anisotropic metamaterials, and Finite Elements simulations.

I. INTRODUCTION

Novel metamaterials^{1,2}, in particular those for which the spatial distribution of optical parameters can be specifically tailor-made, have proven to be a viable route to realize various linear, nonlinear or tunable optical properties and processes. Amongst them, the hyperbolic metamaterials (HM) - indefinite metamaterials, for which the permittivity and permeability tensors are negative along only certain of the principal axes of the metamaterial³ - attract interest because of possibilities of optical steering and manipulation. Closely related are optical effects like negative refraction^{4,5}, hyperlensing⁶⁻⁹, cancellation of reflection and transmission¹⁰. Optical devices based on indefinite media are designed, like, e.g., polarization beam splitters¹¹, angular filters¹², optical transmission modulator¹³. Theoretical approaches were worked out to handle the negative refraction in anisotropic indefinite media have also been presented^{4,14,15}.

Tunability and simple production become important requirements. One of the few metamaterials which offer tunability¹⁶, is nematic liquid crystal (NLC) doped with coated core-shell spheres (NDLC)¹⁷. Recently we have demonstrated a negative refraction in near infra-red (IR) in this system with a planar NLC configuration for a wide interval of incident angles of electromagnetic (EM) wave, using finite elements (FE) calculations (Comsol)¹⁸. Similar results in visible light range were presented in Ref.¹⁹ where it was shown that a HM consisting of NLC doped with a sufficiently high concentration of silver nanoparticles can become a HM; all-angle negative refraction for homeotropic NLC orientation was demonstrated based on geometric arguments.

The point we would like to emphasize here is that a medium is indefinite is neither necessary^{20,21} nor a sufficient condition for negative refraction; we shall show below that for a HM a positive refraction as well as reflection can take place. Thus, additional quantitative

calculations are necessary to trace the path of EM in an indefinite medium.

The aim of this paper is to design, using effective medium approximation and FE calculations, an electric field driven device for switching in NDLC HM between three scenarios: negative refraction, positive refraction and reflection for wide intervals of angles of incidence of EM and of NLC director orientations. To this end, the approach based on negative refraction in anisotropic metamaterials^{14,15} is used.

II. NDLC AS A TUNABLE INDEFINITE MEDIUM

Consider a rectangular NLC cell with thickness L along x direction, filled with NDLC metamaterial described below, with planar alignment of NLC molecules in $x - y$ plane (Fig. 1(a)). The incident light with transverse magnetic (TM) polarization (\vec{E} in $x - y$ plane and \vec{B} along z direction) propagates in $x - y$ plane and impinges as an extraordinary wave onto the NLC host. The permittivity tensor for NLC reads²²:

$$\epsilon_{LC} = \begin{pmatrix} \epsilon_{\perp} + \Delta\epsilon \cos^2 \gamma & \Delta\epsilon \sin \gamma \cos \gamma & 0 \\ \Delta\epsilon \sin \gamma \cos \gamma & \epsilon_{\perp} + \Delta\epsilon \sin^2 \gamma & 0 \\ 0 & 0 & \epsilon_{\perp} \end{pmatrix}, \quad (1)$$

where γ denotes the angle between the $+x$ axis and the director \vec{n} , $\Delta\epsilon = \epsilon_{\parallel} - \epsilon_{\perp}$, $\epsilon_{\parallel} = n_e^2$, $\epsilon_{\perp} = n_o^2$.

The NDLC metamaterial¹⁷ comprises the host nematic liquid crystal containing uniformly distributed non-magnetic spheres with core radius r_1 , made of polaritonic material and semiconductor shell (Drude material) with thickness d . The effective permittivity and permeability of NDLC were calculated in Ref.¹⁷ using Mie theory and Maxwell Garnet mixing rule:

$$\epsilon_{eff} = \epsilon_3 \left(\frac{k_3^3 + 4\pi i N a_1}{k_3^3 - 2\pi i N a_1} \right), \quad \mu_{eff} = \frac{k_3^3 + 4\pi i N b_1}{k_3^3 - 2\pi i N b_1}, \quad (2)$$

where $k_3 = \sqrt{\epsilon_3} 2\pi/\lambda$, λ denotes the free-space wavelength, ϵ_3 - permittivity of the NLC host along main axes, N - number density of the spheres, and a_1, b_1

^{a)}Electronic mail: grzegorz.pawlik@pwr.wroc.pl

– scattering coefficients. Formula (2) is valid in long-wavelength limit for low values of filling factor $f = 4\pi(r_1 + d)^3 N/3$. Parameters used in this paper are: $r_1 = 0.05 \mu\text{m}$, $d = 0.01 \mu\text{m}$, $f = 0.06$, $\varepsilon(\infty) = 17$, $\omega_T/2\pi = 360 \text{ THz}$, $\omega_L/2\pi = 855 \text{ THz}$, $\gamma_1/2\pi = 3.75 \text{ THz}$, $\omega_p\pi = 230 \text{ THz}$, $\gamma_2 = \omega_p/60$, $\lambda = 1.75 \mu\text{m}$, see Ref.¹⁷ for the definitions. Plots of the real parts $\varepsilon'_{eff} = \Re\{\varepsilon_{eff}\}$, $\mu'_{eff} = \Re\{\mu_{eff}\}$ in function of ε_3 are shown in Fig. 1(b).

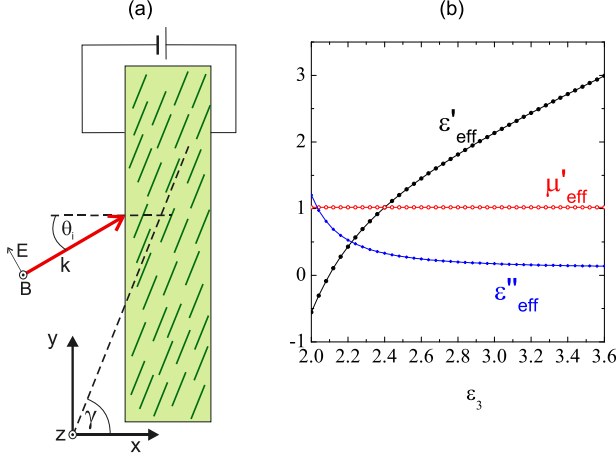


FIG. 1. (Color online) (a) Geometry of the system. (b) Dependence of effective permittivity and permeability on permittivity of the LC host ε_3 , Eq. (2).

The propagation of a TM incident wave in this medium can be described by specifying ε'_{eff} in the propagation plane along principal axes and $(\mu'_{eff})_{zz}$ ⁴. Those components were calculated from Eq. (2) using the tensor components of ε_3 along main axes: ε_{\parallel} and ε_{\perp} ²³. In this paper we put $\varepsilon_{\perp} = 2$, $\varepsilon_{\parallel} = 2.91$. Then, $(\varepsilon'_{eff})_{\perp} \simeq -0.52$ for $\varepsilon_3 = \varepsilon_{\perp}$ and $(\varepsilon'_{eff})_{\parallel} \simeq 2$ for $\varepsilon_3 = \varepsilon_{\parallel}$. As the real parts of effective permittivities along principal axes are opposite in signs, NDLC is an indefinite medium. The effective permeability is independent on ε_3 in the interval of values relevant for this design (Fig. 1(b)) and we put $(\mu'_{eff})_{zz} \equiv \mu'_{eff} \simeq 1$.

The tensor components $(\varepsilon'_{eff})_{xx}$, $(\varepsilon'_{eff})_{yy}$, $(\varepsilon'_{eff})_{xy}$ in coordinates from Fig. 1(a), calculated by rotating the diagonal tensor in principal axes around z axis by angle γ , are shown in Fig. 2. As angle γ characterizes the direction of the optic axis which can be varied through the external electric field, we conclude that the NDLC becomes (within the limits of validity of the effective medium theory) a tunable hyperbolic medium.

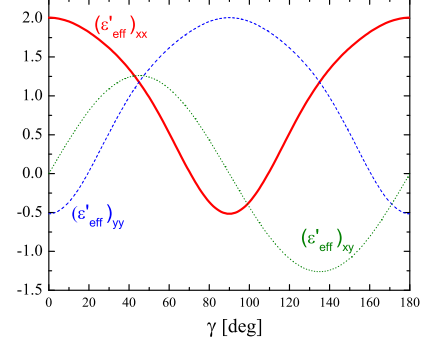


FIG. 2. The dependence of tensor components $(\varepsilon'_{eff})_{xx}$, $(\varepsilon'_{eff})_{yy}$ and $(\varepsilon'_{eff})_{xy}$ on rotation angle γ .

III. REFRACTION ON THE BOUNDARY ISOTROPIC/INDEFINITE MATERIAL. ALL-ANGLE NEGATIVE REFRACTION

Rotation of the director of NLC accompanied by the variation of the effective permittivity tensor changes the refraction at the boundary isotropic/indefinite medium. In geometric approach this rotation promotes the rotation of the hyperbola of equifrequency contour in NDLC material¹⁴. In the principal axes of effective permittivity tensor this hyperbola determines the dispersion relation for TM waves in NDLC²:

$$\frac{k_x^2}{(\varepsilon'_{eff})_{yy}} + \frac{k_y^2}{(\varepsilon'_{eff})_{xx}} = \frac{\omega^2}{c^2}, \quad (3)$$

where c denotes the velocity of light in vacuum. The case of $\gamma = 90^\circ$ is shown as inset in Fig. 3, where the equifrequency contour of an isotropic material is represented by a circle. Based on this diagram, the geometrical analysis of refraction can be done in a standard way¹⁴ by observing the continuity of the tangential components of incident (\vec{k}_i) and refracted (\vec{k}_r) wave vectors. The direction of energy flow described by the Poynting vector \vec{S} within the indefinite medium is indicated by the arrow drawn normal to the hyperbolic isofrequency surface. The refraction angles for the wave beam $\theta_{r,S}$ and for the wave vector $\theta_{r,k}$ can be calculated analytically. The same geometric approach is used in the case of rotated nematic/equifrequency contour (see, e.g., appendix in Ref.¹⁴).

In the case of uniform configuration of NLC ($\gamma = 90^\circ$) the geometric approach predicts that negative refraction of the TM wave occurs for all angles of incidence θ_i (solid line in Fig. 3). This prediction is confirmed by FE calculations (symbols in Fig. 3). Fig. 4 characterizes the energy flow and electromagnetic wave in the system for angle of incidence $\theta_i = 40^\circ$. Part (a) shows the magnitude of the electric field and Poynting vectors, part (b) – the z -component of magnetic field. Direction of vector

\vec{k}_r for refracted wave and angle of negative refraction for Poynting vector are in agreement with analytical results from Fig. 3.

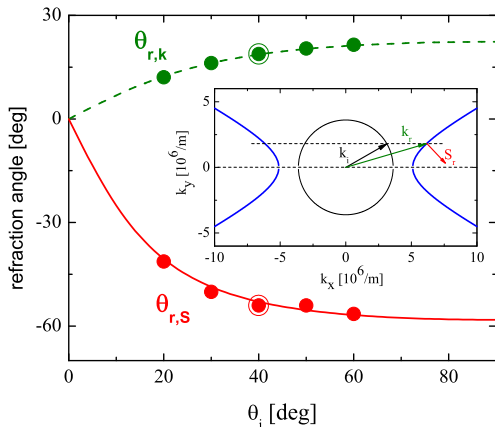


FIG. 3. (Color online) Plots of refraction angles $\theta_{r,s}(\theta_i)$ (solid line) and $\theta_{r,k}(\theta_i)$ (dashed line). Symbols represent FE results¹⁸. Large symbol - see Fig. 4. Inset: isofrequency contours for the TM wave incident from an isotropic material to an indefinite one with $(\epsilon'_{eff})_{xx} < 0$ and $(\epsilon'_{eff})_{yy} > 0$ for the angle of incidence $\theta_i = 30^\circ$.

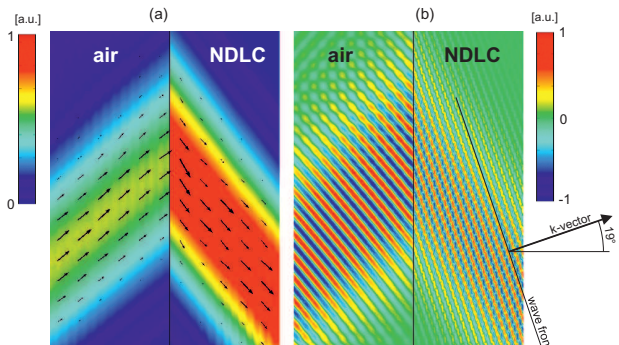


FIG. 4. (Color online) Finite Element simulations of the electric and magnetic field mapping for gaussian beam with TM polarization, $\theta_i = 40^\circ$. Magnitude of the electric field and Poynting vectors (a), z -component of magnetic field (b).

IV. ELECTRIC SWITCH BETWEEN NEGATIVE/POSITIVE REFRACTION AND REFLECTION

Using the formalism presented in the last Section we have studied the behaviour of a plane TM wave incident from vacuum on the indefinite NDLC for a few chosen angles of incidence θ_i and for an arbitrary orientation of NLC director ($0 \leq \gamma \leq 180^\circ$). The dependence of refraction angle $\theta_{r,s}$ on γ is shown in Fig. 5. We have singled out three distinct regions. We first discuss Region II that was calculated using analytical geometric approach and extends from $\gamma = \gamma_N \simeq 64^\circ$ to $\gamma = \gamma_P \simeq 116^\circ$. The

location of its boundaries is independent on θ_i . The negative refraction for the Poynting vector is present for all angles of incidence θ_i , while positive refraction requires that $\theta_i < \theta_{i,0} \approx 50^\circ$. For example, for $\theta_i = 30^\circ$ negative refraction is present for $\gamma_N < \gamma_0 \approx 106^\circ$, positive refraction - for $\gamma > \gamma_0$. We have used the approach from Ref.¹³ to show that in this region the wave vector of the wave propagating in NDLC HM metamaterial is purely real which implies that the plane wave impinging from vacuum excites an homogeneous wave. In regions I ($\gamma < \gamma_N$) and III ($\gamma > \gamma_P$) the geometric construction breaks down, the wave vector becomes imaginary, which implies that the impinging plane wave excites an evanescent wave.

To verify analytical geometric predictions we have used FE calculations. In Regions I and III total reflection occurs (there was no transmitted wave) while in Region II the simulations for $\theta_i = 30^\circ$ (symbols) confirm theoretical analysis. Small discrepancies close to boundaries of Region II have numerical origin.

These results make possible a design of a novel electrooptic effect: external electric field driven real time switch between negative refraction, positive refraction and total reflection. To illustrate its functionality we have performed FE simulations of a TM gaussian beam with $\lambda_0 = 1.74 \mu\text{m}$ impinging a NDLC HM cell with thickness $10 \mu\text{m}$ at angle of incidence $\theta_i = 30^\circ$. In Fig. 6 the magnetic field mapping is shown for three operating states of the switch, which depend on the orientation of the NLC host controlled by external electric field: negative refraction for $\gamma = 90^\circ$ (top); positive refraction for $\gamma = 110^\circ$ (middle) and total reflection for $\gamma = 0^\circ$ (bottom).

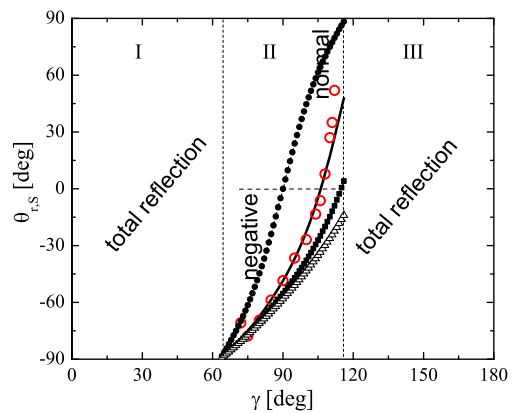


FIG. 5. Refraction angle $\theta_{r,s}$ in function of the orientation γ of NLC director for $\theta_i = 0^\circ$ (full circles), 30° (solid line), 50° (squares) and 80° (triangles). Large circles represent FE calculations for $\theta_i = 30^\circ$.

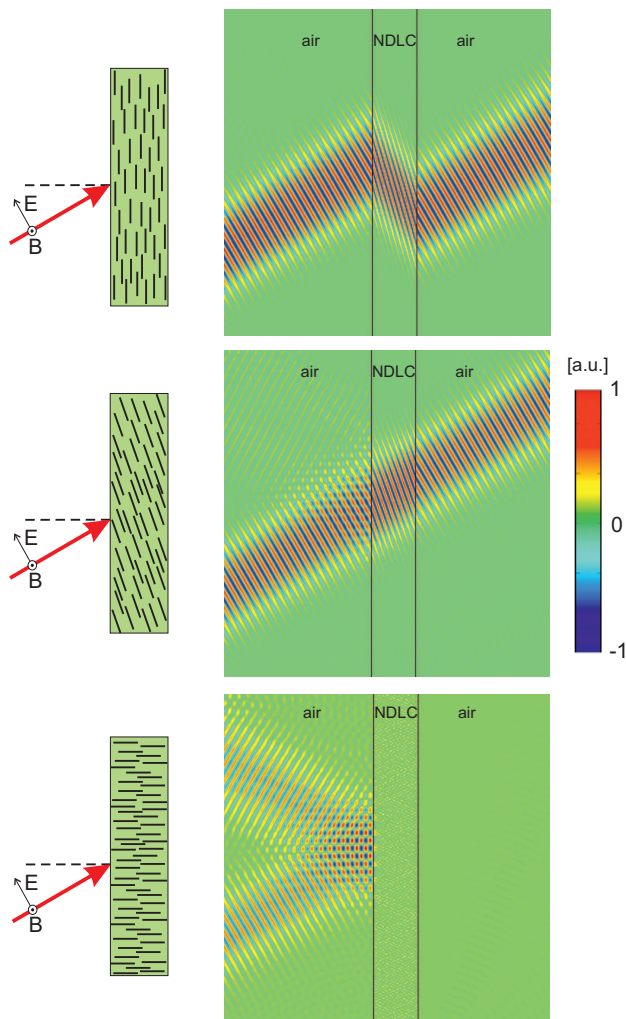


FIG. 6. (Color online) Operating principle of the switch. Left: orientation of NLC host, right: magnetic field mapping for a gaussian TM beam incident at $\theta_i = 30^\circ$. Negative refraction ($\gamma = 90^\circ$, top); positive refraction ($\gamma = 110^\circ$, middle); total reflection ($\gamma = 0^\circ$, bottom).

V. CONCLUSIONS

We have shown using effective medium approach and FE calculations (Comsol) that nanosphere dispersed liquid crystal metamaterial becomes a tunable indefinite medium in near IR. The tunability is provided by varying the external electric field which changes the orientation of the NLC director, the overall effective permittivity tensor and the orientation of the hyperbola of the dispersion relation of extraordinary waves through the medium. The latter allows to control the character of electromagnetic field in the medium: propagating or

evanescent. We have exploited this tunability to design a new electrooptic effect for the manipulation of light: electric field driven switch between negative and positive refraction and reflection, and have illustrated its functionality. Compared to negative refraction in pure NLC medium^{20,21} the NDLC device operates in much wider intervals of incidence/refraction angles.

Acknowledgements

This work is supported by the Air Force Office of Scientific Research (AFOSR). G.P. thanks Polish National Science Centre for financial support under Grant NN507 322440. K.T. acknowledges support of the Foundation for Polish Science START Program.

- ¹N. Engheta and R. W. Ziolkowski, *Metamaterials: Physics and Engineering Explorations* (Wiley, Hoboken, 2006).
- ²W. Cai and V. Shalaev, *Optical Metamaterials Fundamentals and Applications* (Springer, 2010).
- ³D. R. Smith and D. Schurig, Phys. Rev. Lett. **90**, 077405 (2003).
- ⁴D. R. Smith, P. Kolinko, and D. Schurig, J. Opt. Soc. Am. **B21**, 1032-1043 (2004).
- ⁵A. Fang, T. Koschny, and C. M. Soukoulis, Phys. Rev. **B79**, 245127 (2009).
- ⁶Z. Jacob, L. V. Alekseyev, and E. Narimanov, Opt. Express **14**, 8247-8256 (2006).
- ⁷H. Lee, Z. Liu, Y. Xiong, C. Sun, and X. Zhang, Opt. Express **15**, 15886-15891 (2007).
- ⁸J. Yao, K. T. Tsai, Y. Wang, Z. Liu, G. Bartal, Y.L. Wang, and X. Zhang, Opt. Express **17**, 22380-22385 (2009).
- ⁹B. D. F Casse, W. T. Lu, Y. J. Huang, E. Gultepe, L. Menon, and S. Sridhara, Appl. Phys. Lett. **96**, 0231114 (2010).
- ¹⁰J. Yang, X. Hu, X. Li, Z. Liu, X. Jiang, and J. Zi, Opt. Lett. **35**, 16-18 (2010).
- ¹¹J. Zhao, Yan Chen, and Y. Fen, Appl. Phys. Lett. **92**, 071114 (2008).
- ¹²L. V. Alekseyev, E. E. Narimanov, T. Tumkur, H. Li, Yu. A. Barnakov, and M. A. Noginov, Appl. Phys. Lett. **97**, 131107 (2010).
- ¹³E. Spinozzi and A. Ciattoni, Opt. Mat. Express **1**, 732-741 (2011).
- ¹⁴T. M. Grzegorzczuk, M. Nikku, X. Chen, B.-I. Wu, and J. Au Kong, IEEE Transactions on Microwave Theory and Techniques, **53**, 1443-1450 (2005).
- ¹⁵S.-H. Liu and L.-X. Guo, Progress In Electromagnetics Research, **115**, 243-257 (2011).
- ¹⁶G. Pawlik, M. Jarema, W. Walasik, A. C. Mitus, and I. C. Khoo, J. Opt. Soc. Am. B **27**, 567-576 (2010).
- ¹⁷I. C. Khoo, D. H. Werner, X. Liang, A. Diaz, and B. Weiner, Opt. Lett. **31**, 2592-2594 (2006).
- ¹⁸G. Pawlik, W. Walasik, K. Tarnowski, A.C. Mitus, and I. C. Khoo, Proc. of SPIE **8828**, 88280E (2013); **8901**, 890111 (2013).
- ¹⁹D. Jia, C. Yang, X. Li, Z. Peng, Y. Liu, Z. Cao, Q. Mu, L. Hu, D. Li, L. Yao, X. Lu, X. Xiang, H. Zhang, and L. Xuan, Liquid Crystals (2013), DOI: 10.1080/02678292.2013.847126
- ²⁰D. Jia, C. Yang, Z. Peng, X. Li, Y. Liu, L. Yao, Z. Cao, Q. Mu, L. Hu, X. Lu and L. Xuan, Liquid Crystals **40**, 599-604 (2013).
- ²¹O. P. Pishnyak and O. D. Lavrentovich, Appl. Phys. Lett. **89**, 251103 (2006).
- ²²X. Wang, D.H. Kwon, D.H. Werner, I.C. Khoo, A. V. Kildishev and V. M. Shalaev, Appl. Phys. Lett. **91**, 143122 (2007).
- ²³G. Pawlik, K. Tarnowski, W. Walasik, A. C. Mitus, and I. C. Khoo, Opt. Lett. **37**, 1847-1849 (2012).